

RSC Advances



This is an *Accepted Manuscript*, which has been through the Royal Society of Chemistry peer review process and has been accepted for publication.

Accepted Manuscripts are published online shortly after acceptance, before technical editing, formatting and proof reading. Using this free service, authors can make their results available to the community, in citable form, before we publish the edited article. This *Accepted Manuscript* will be replaced by the edited, formatted and paginated article as soon as this is available.

You can find more information about *Accepted Manuscripts* in the [Information for Authors](#).

Please note that technical editing may introduce minor changes to the text and/or graphics, which may alter content. The journal's standard [Terms & Conditions](#) and the [Ethical guidelines](#) still apply. In no event shall the Royal Society of Chemistry be held responsible for any errors or omissions in this *Accepted Manuscript* or any consequences arising from the use of any information it contains.

1 Modeling of Thermal Conductivity of Nanofluids Considering Aggregation and
2 Interfacial Thermal Resistance

3

4 Meng Liu^a, Chen Ding^{a*}, Jun Wang^a

5 ^aSchool of Aeronautic Science and Engineering, Beijing University of Aeronautics
6 and Astronautics, Beijing 100191, China

7 *Corresponding author. Tel: +86-132-4130-1892

8 E-mail address: dingchen@buaa.edu.cn (C. Ding)

9

10 **Abstract**

11 A model with the consideration of particle size, aggregate size and interfacial thermal
12 resistance is developed to predict the thermal conductivity of nanofluids. Interfacial
13 thermal resistance is modeled to have relationship with the equivalent particle size in
14 terms of keeping thermal resistance constant. The shape factor of aggregate is
15 determined by the number of particles in the aggregate. The present model agrees well
16 with the wide accepted experimental data. It concludes that particle size and aggregate
17 size have positive effect on the thermal conductivity enhancement, since the increase
18 of particle size can weaken the effect of interfacial thermal resistance, and the
19 increase of aggregate size can offer fast heat transfer path for adjacent particles and it
20 significantly increases the shape factor of aggregate. The thermal conductivity of
21 nanofluids increases linearly with particle volume fraction and the increase rate differs
22 according to particle size and aggregate size. The inferred values of interfacial thermal
23 resistance are in a reasonable range and fit well with different experimental data. If
24 the particle volume fraction is lower than 0.1% or the particle size is smaller than 10
25 nm without aggregation, the factors of nano-convection and nanolayer need to be
26 taken into account.

27 **Key words**

28 Nanofluids, Thermal conductivity, Theoretical model, Aggregate size, Interfacial
29 thermal resistance

30

31 1. Introduction

32 The discovery of nanofluids, in which solid nanoparticles disperse in
33 conventional base fluid, has aroused the interests worldwide in the last two decades.
34 Numerous studies showed that, compared with base fluid, nanofluids can dramatically
35 improve thermal conductivity, convective heat transfer and solar energy absorption
36 features.¹⁻³

37 Reports showed that the thermal conductivity, k , of nanofluids depended on
38 factors like particle volume fraction (ϕ), single particle diameter (d), particle
39 morphology, additives, pH value, temperature, nature of the base fluid and particle
40 materials etc.⁴ The studies of the effect of particle size on the k of nanofluids
41 concluded conflicting reports. Patel et al.⁵ and Cui et al.⁶ used experimental method
42 and the molecular dynamics (MD) simulations respectively to find out that the k
43 increased with the reduction of particle diameter. However, Beck et al.⁷ measured the
44 k of nanofluids that contain nanoparticles of different diameters and found an
45 enhancement in k as particle size increased. Considering temperature, most studies
46 showed an enhancement in k with the increase of temperature.^{5,8,9} Taking the materials
47 of base fluid and nanoparticles into account, most of the studies showed an increase in
48 k with the reduction of k of the base fluid and the increase of k of the nanoparticles.^{5,10}
49 The shape of particles and the forming of clusters in nanofluids significantly
50 influenced the k of nanofluids. The benchmark study on alumina nanoparticles and
51 nanorods in PAO showed that the k was higher if the particles have larger aspect ratio
52 (nanorods).¹ Particles in the nanofluids were prone to form aggregates, and the
53 reason why aggregates can enhance the k of nanofluids was because aggregates
54 created paths of lower thermal resistance among particles and heat could conduct
55 rapidly in the cluster. What is more, aggregates set up percolating structures and the
56 effective volume of aggregates could be much larger than the total volume of
57 particles.^{12,13} The factors of pH value and the addition of surfactant on k were also
58 studied. Lee et al.¹⁴ found that since the pH value was far from the isoelectric point,
59 the particle size changed and particles became more stable. Younes et al.¹⁵

60 demonstrated that the pH value affected zeta potentials and aggregate size, and
61 surfactant could separate particles to avoid forming clusters and stabilize nanofluids.

62 The mechanisms of the unusual high thermal conductivity of nanofluids with low
63 particle volume fraction are controversial. Maxwell model was firstly introduced to
64 model the k of nanofluids based on the effective medium theory (EMT).¹⁶ Hamilton¹⁷
65 took particles shape effects into account. The phenomenon that the measured k of
66 nanofluids was anomalously greater than theoretical predictions attracted considerable
67 attentions.¹ The existence of an ordered layer of liquid molecules at the solid-liquid
68 interface was experimentally proved, and it could measurably increase the k of
69 nanofluids when particle diameter was below 10 nm.^{18,19} Brownian motion and the
70 convective heat transfer induced by Brownian motion of nanoparticles were
71 considered as the mechanisms of the enhancement of k in nanofluids.²⁰⁻²² On the
72 contrary, Gao et al.²³ measured the k of nanofluids in both liquid and solid states and
73 figured that the effect of Brownian motion on k of nanofluids was much less than that
74 of the clustering formation.

75 Mathematical models to predict the k of nanofluids are built on many
76 investigations. Brownian motion of particles may result in convection-like effects on
77 the nanoscale.²⁴ Prasher et al.²¹ introduced a model considering local convection
78 caused by Brownian movement of particles based on EMT. The factor of convection
79 was given $k_{con} = (1 + A Re^m Pr^{0.333} \phi) k_f$, where Re and Pr are Reynolds number and
80 Prantl number respectively, and A and m are constants determined by experimental
81 results. Yu et al.¹⁹ modified the Maxwell model to include the effect of the ordered
82 nanolayer. With the nanolayer of thickness h attaching to the surface of particles, the
83 equivalent particle radius became $r+h$ and the equivalent particle volume fraction
84 increased. The effect of the ordered layer was rapidly weakened as particle diameter
85 increased and it wore off if particle diameter was larger than 10 nm. Increasing
86 evidence suggests that EMT can estimate thermal conductivity considering the effect
87 of aggregation and interfacial resistance.^{10,25} Based on the study of Nan et al.²⁶ who
88 introduced a methodology to predict the k of particulate composites with interfacial

89 thermal resistance, Prasher et al.¹² and Evans et al.²⁷ built a three-level
90 homogenization model to evaluate the k of colloids, assuming that an aggregate was
91 composed of a few linear chains that span the whole cluster and side chains. In the
92 first level, the k of aggregate with dead end was calculated by Bruggeman model, then
93 the k of the aggregate that includes a backbone was calculated by the model of Nan et
94 al. Finally, the k of nanofluids with aggregates was obtained by Maxwell model.
95 Based on the three-level homogenization, Okeke et al.²⁸ numerically investigated the
96 k of nanofluids with the consideration of different factors and found that aggregate
97 size affected thermal conductivity while interfacial thermal resistance did not play the
98 major role. Zhou et al.²⁹ built a model based on particle size distribution and found
99 that the k of nanofluids could be enhanced with clusters in it.

100 In this paper, the authors build a model to predict the k of nanofluids based on the
101 EMT, considering the factor of particle size, aggregate size, particle volume fraction
102 and interfacial thermal resistance. According to this model, the increase of interfacial
103 thermal resistance is equivalent to the decrease of particle size in terms of keeping
104 thermal resistance constant, which further affects the effective particle volume
105 fraction. Aggregate size affects the shape factor and the number of particles in the
106 aggregate. Then the predictions of present model are compared with experimental
107 results in the literature and they are in good agreement. After that, various simulations
108 of the k of nanofluids are established to analyze factors such as particle size,
109 aggregate size and particle volume fraction on the k of nanofluids. Finally, further
110 discussion on the divergence of present model and some experimental data is made.

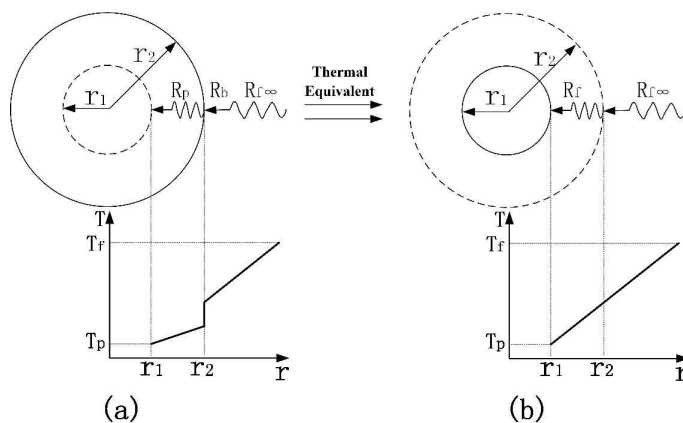
111 2. Model development

112 The schematic of a particle in nanofluids is shown in Fig. 1. The particle is
113 assumed to be sphere and has a radius of r_2 . The thermal resistance in nanofluids
114 contains particle thermal resistance $R_p(K/W)$, fluid thermal resistance $R_f(K/W)$
115 and interfacial thermal resistance $R_b(Km^2/W)$ at the solid/liquid interface. The
116 boundary conditions at the interface can be expressed as³⁰

$$k_p \frac{\partial T_p}{\partial r} = k_f \frac{\partial T_f}{\partial r}, \quad (1)$$

$$T_p - T_f = -k_p R_b \frac{\partial T_p}{\partial r}, \quad (2)$$

where k_p and k_f are particle and base fluid thermal conductivity (W/mK) respectively, T_p and T_f are particle temperature and base fluid at the solid/liquid interface, and r refers to radius vector.



The schematic of the geometry of a particle. The circle with solid line shows (a) the actual particle and (b) the thermal equivalent particle. The temperature change along the radius direction when assuming there is temperature gradient around a particle is also presented. Nomenclature $R_{f\infty}$ refers to water thermal resistance around the particle.

Considering that there is temperature gradient around a particle, as shown in Fig. 1, temperature difference exists at the solid/liquid interface due to interfacial thermal resistance. Since temperature difference makes it difficult to model the process of heat conduction, we assume that there is no temperature difference at the solid/liquid interface and particle radius is smaller than r_2 , as depicted in Fig. 1(b). We can get certain value of hypothetical particle radius r_1 that make the hypothetical particle thermal resistance (Fig. 1(b)) equal to the original particle thermal resistance (Fig. 1(a)).

136 The thermal resistance of the sphere between the surfaces of radius r_1 and r_2
 137 that contains interfacial thermal resistance can be expressed as

$$138 \quad R = \frac{1}{4\pi k_p} \left(\frac{1}{r_1} - \frac{1}{r_2} \right) + \frac{R_b}{4\pi r_2^2}. \quad (3)$$

139 Assuming that there is no interfacial thermal resistance at the solid/liquid
 140 interface and particle radius is r_1 , as shown in Fig. 1(b), the space between r_1 and r_2
 141 is filled with liquid, so the thermal resistance between the surfaces of radius r_1 and
 142 r_2 becomes

$$143 \quad R' = \frac{1}{4\pi k_f} \left(\frac{1}{r_1} - \frac{1}{r_2} \right). \quad (4)$$

144 Then we can get certain value of r_1 that makes the thermal resistance in Fig. 1(a)
 145 and Fig. 1(b) be equal. If so, the thermal resistance of the original particle and the
 146 hypothetical particle are the same, which is called “thermal equivalent condition”. In
 147 this condition we can get

$$148 \quad \frac{R_b}{4\pi r_2^2} + \frac{1}{4\pi k_p} \left(\frac{1}{r_1} - \frac{1}{r_2} \right) = \frac{1}{4\pi k_f} \left(\frac{1}{r_1} - \frac{1}{r_2} \right). \quad (5)$$

149 Transforming Eq. 5, r_1 is expressed as

$$150 \quad r_1 = \frac{(k_p - k_f)r_2^2}{(k_p - k_f)r_2 + R_b k_p k_f}. \quad (6)$$

151 Considering the particle in Fig. 1(b), the effective particle volume fraction can be
 152 expressed as

$$153 \quad \phi_{eff} = \frac{r_1^3}{r_2^3} \phi, \quad (7)$$

154 where ϕ is the particle volume fraction. Interfacial thermal resistance reduces the
 155 equivalent particle radius and the effective particle volume fraction.

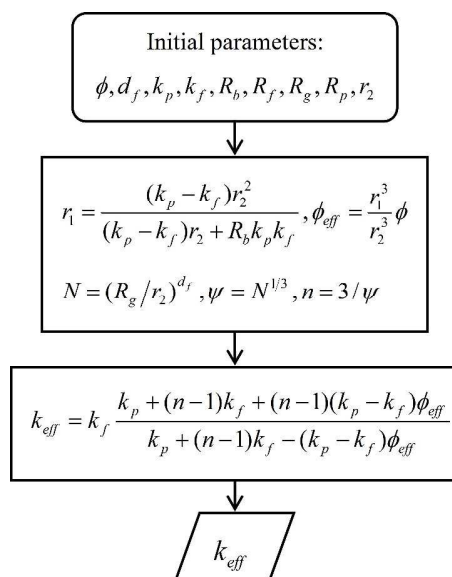
156 Hamilton¹⁷ developed a model to predict the effective thermal conductivity of
 157 suspensions based on EMT. The influence of irregular shapes of particles was

158 considered and the expression of the k of nanofluids was given:

$$159 \quad k_{eff} = k_f \frac{k_p + (n-1)k_f + (n-1)(k_p - k_f)\phi_{eff}}{k_p + (n-1)k_f - (k_p - k_f)\phi_{eff}}, \quad (8)$$

160 where k_{eff} is the effective thermal conductivity of nanofluids, n is the shape factor
 161 given by $n = 3/\psi$ with ψ denoting the sphericity of particles. ψ is defined as the
 162 ratio of the surface area of the sphere with the same volume as a particle to the
 163 external surface area of a particle. In present model, the effective thermal conductivity
 164 of nanofluids can be determined by Eq. 8.

165 Due to Brownian move and the interaction among particles, particles are
 166 randomly packed together and form aggregates of fractal structure.³¹⁻³³ The number of
 167 particles in an aggregate, N , is given by $N = (R_g/r)^{d_f}$, where R_g is the aggregate
 168 radius of gyration, and d_f is the aggregate fractal dimension. As previously denoted,
 169 an aggregate act as an independent unit of particle and its surface area is the same as
 170 the surface area of primary particles in the aggregate. So assuming that the primary
 171 nanoparticles are spheres with uniform size, we can get $\psi = N^{1/3}$ according to the
 172 definition of ψ . The block diagram for the guidance of the model usage is shown in
 173 Fig. 2.



174

175

Fig. 2. Block diagram of the step of model

176 3. Model verification

177 The comparisons between the present model and experimental results in the
178 literature are used to validate the present model. The sizes of particles and aggregates
179 are rarely mentioned in literature, and results vary when using different measurement
180 methods for the same sample because of possible size polydispersity, formation of
181 ordered fluid layers and clustering of particles.^{7,34}

182 Since particle size is defined by the area of the solid/liquid interface that acts as a
183 new phase affecting properties of nanofluids, the specific surface area of the particles
184 measured by Brunauer- Emmett- Teller (BET) can be used to determine average
185 particle size. The average hydrodynamic diameter of species involved in Brownian
186 motion can be estimated by dynamic light scattering (DLS). Since one aggregate
187 involves in Brownian motion as a whole, the average aggregate size can be
188 determined by DLS. In these considerations, the reported particle sizes using BET and
189 DLS are used to determine particle size and aggregate size, and the experimentally
190 measured k of nanofluids are used to validate the present model.

191 The interfacial thermal resistance at the solid/liquid interface has been discussed
192 by researchers. Wilson et al.³⁵ experimentally estimated $R_b \approx 0.77 \times 10^{-8} \text{ Km}^2/\text{W}$ for
193 pt/water interface and got $R_b \approx 1.61 \times 10^{-8} \text{ Km}^2/\text{W}$ for particle-water interface based on
194 diffuse-mismatch model (DMM). Xue et al.³⁶ figured that interfacial thermal
195 resistance was strongly dependent on the type of bonding between the solid and the
196 liquid, and nanofluids characterized by weak atomic bonding at the solid- liquid
197 interfaces will exhibit high thermal resistance. According to DMM, the velocity of
198 sound and the heat capacity of the base fluid have influence on the interfacial thermal
199 resistance. Under the assumption that the velocity of sound in ethylene glycol and
200 water were approximately the same, Prasher et al.²¹ assumed
201 $R_b \approx 1.21 \times 10^{-8} \text{ Km}^2/\text{W}$ for ethylene glycol based nanofluids. Since the accurate value
202 of R_b for different particle- liquid interface is unavailable, we assume
203 $R_b = 1 \times 10^{-8} \text{ Km}^2/\text{W}$ for particle- water interface, and $R_b = 1.5 \times 10^{-8} \text{ Km}^2/\text{W}$ for

204 particle- organic solvent interface based on DMM as a first approximation.

205 The coagulation of primary particles into aggregates, known as “cluster-cluster”
 206 aggregation, can be characterized by fractal dimension d_f . Two kinetic regimes,
 207 diffusion-limited aggregation (DLA) and reaction-limited aggregation (RLA), have
 208 been identified for cluster-cluster aggregation.³¹ In DLA, particles collide and
 209 combine instantaneously, producing a highly porous, convoluted aggregate, which is
 210 similar to the process of aggregation in nanofluids. The value of d_f is around
 211 1.8.³¹⁻³³ In RLA, there is a significant repulsive barrier to aggregation and the sticking
 212 probability on aggregate-aggregate interaction is less than unity. The value of d_f is
 213 around 2.1-2.2.³¹ So it is reasonable to assume $d_f = 1.8$ in this paper.

214 The thermal conductivity of four sets of test nanofluids were measured by over 30
 215 organizations worldwide to resolve the inconsistencies of the reported thermal
 216 conductivity of nanofluids.¹¹ Since the data from most organizations are lied within a
 217 narrow band, these data are used to validate the present model. The characteristics of
 218 the four sets of samples are listed in Table 1. In the present model, particles are
 219 assumed to be sphere, so the samples of alumina nanorods are not used for
 220 comparison.

221 Table 1. Characteristics of the samples for validation

	Particle type	Volume fraction (%) ^a	Particle size (nm) ^b	Aggregate size (nm) ^c	Type Base fluid
1	Alumina	1	10	81.5	PAO+surfactant
2	Alumina	3	10	105.5	PAO+surfactant
3	Gold	0.001	15	15	Water+stabilizer
4	Silica	31.1	22	22	Deionized water
5	Mn-Zn	0.17	7.4	11	Water+stabilizer

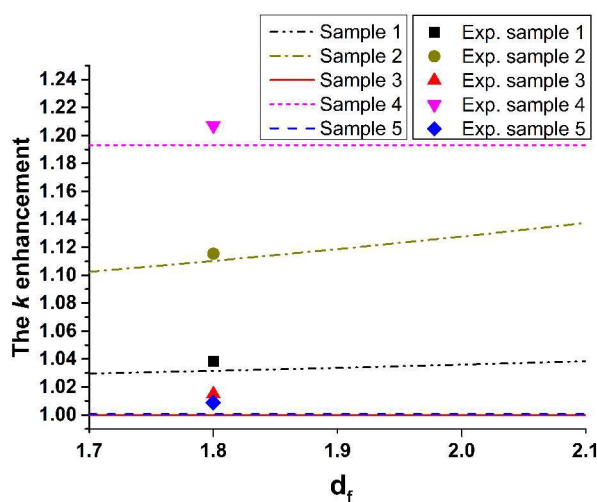
222 ^aThe volume fraction of particles are reported by the providers.

223 ^bThe particle sizes are the nominal particle sizes. As gold particles and Silica particles
 224 are well dispersed without aggregation, the particle sizes are the same as aggregate

225 sizes.

226 °The sizes of aggregates are the average sizes of dispersed phase, measured by DLS,
227 or the particle size for the nanofluids without aggregation.

228 Comparisons of the k enhancement (k_{eff}/k_f) between experimental results and
229 predictions of the present model are depicted in Fig. 3. The k enhancement as a
230 function of fraction dimension is plotted to evaluate the robustness of the model since
231 the value of fraction dimension (d_f) is picked by hand after referring to some
232 references.



233
234 Fig. 3. The k enhancement as a function of fractal dimension. The k enhancement of
235 experimental results from Ref. 11 are also presented.

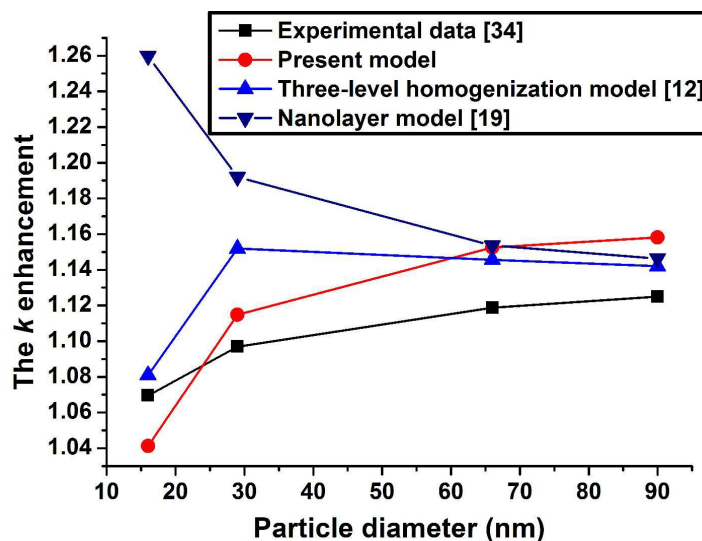
236 It shows that the experimental data is consistent with the present model if the
237 fraction dimension is set as 1.8. The influence of the magnitude of the fraction
238 dimension on the k enhancement are minor enough to prove that the agreement is
239 truly convincing. Besides, the volume fraction of gold particles is too low to estimate
240 the k enhancement using present model.

241 4. Results and discussions

242 4.1 Effect of particle size on the k enhancement of nanofluids

243 The predictions of the k enhancement with different particle sizes using present
244 model, three-level homogenization model,¹² and the renovated Maxwell model that
245 considers nanolayer¹⁹ are shown in Fig. 4. The experimental data measured by

246 Timofeeva et al.³⁴ are also listed for comparison. They measured the k of water-based
 247 α -SiC nanofluids for different particle sizes. The average particle diameters are
 248 determined by BET and the average aggregate sizes are measured by DLS. The
 249 parameters in the three-level homogenization model are the same as the proposed
 250 values in ref. 12. The particle sizes and aggregate sizes used in Fig. 4 are the same as
 251 the experimental measurements.



252
 253 Fig. 4. Dependence of the k enhancement on the average particle diameter in 4.1 vol%
 254 water based SiC nanofluids. The experimental data in ref. 34 and predictions obtained
 255 by the present model, the three-level homogenization model, and the renovated
 256 Maxwell model that considers nanolayer are presented.

257 Fig. 4. indicates that both the present model and the experimental results show the
 258 increase of k enhancement with the rise of average particle sizes. The reason why
 259 particle size has positive effect on k enhancement is that as the average particle size
 260 increases, the total surface area of the solid/liquid interface decreases geometrically,
 261 thus weakening the effect of interfacial thermal resistance (according to Eq. 3). The
 262 predictions of this model (k_{cal}) fit well with the experimental results (k_{exp}) with the
 263 deviations $((k_{cal} - k_{exp})/k_{exp} \times 100\%)$ within $\pm 3\%$.

264 For the three-level homogenization model, although the increase of particle size
 265 can weaken the effect of interfacial thermal resistance and enhance the k of nanofluids,
 266 the aggregate size has greater impact on the k of nanofluids. It also shows that

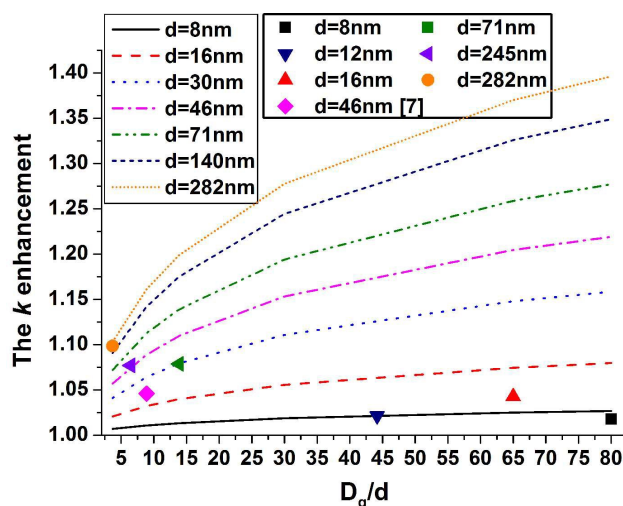
267 compared with the three-level homogenization model, the present model can better
268 predict the k of nanofluids. According to the renovated Maxwell model, the nanolayer
269 has significant impact on small particles. However, with the increase of particle sizes,
270 the k enhancement decreases and the renovated Maxwell equation reduces to the
271 original Maxwell equation, because the impact of nanolayer becomes smaller.

272 **4.2 Effect of aggregate size on the k enhancement**

273 Studying the k enhancement with absolute value of aggregate size is meaningless
274 because particle sizes vary. In this consideration, the authors investigate the effect of
275 relative aggregate size, defining as the ratio of aggregate diameter to particle diameter
276 (D_g/d), on the k enhancement. The relative aggregate size reflects the amount of
277 particles of an aggregate and its aggregate shape factor.

278 The k enhancement as the function of D_g/d for water based alumina nanofluids
279 is shown in Fig. 5. The particle volume fraction is set as 2% and the particle diameters
280 are kept constant for each line. The k of 2 vol% water based alumina nanofluids
281 reported by Beck et al.⁷ are also presented to make a comparison. The particle
282 diameters were from BET measurement and the aggregate sizes were from DLS.

283 Fig. 5. shows that the k enhancement rises rapidly as D_g/d increases, and the
284 growth rate decreases as aggregate size becomes larger. If the aggregate size is fixed,
285 k enhancement increases as particle size becomes larger. The estimates of the present
286 model show a good agreement with the experimental data, with deviations
287 within 4.67% .



288

289 Fig. 5 Influences of relative aggregate size (D_g/d) on the k enhancement of 2 vol%

290 water based alumina nanofluids. Experimental data from ref. 7 are also presented.

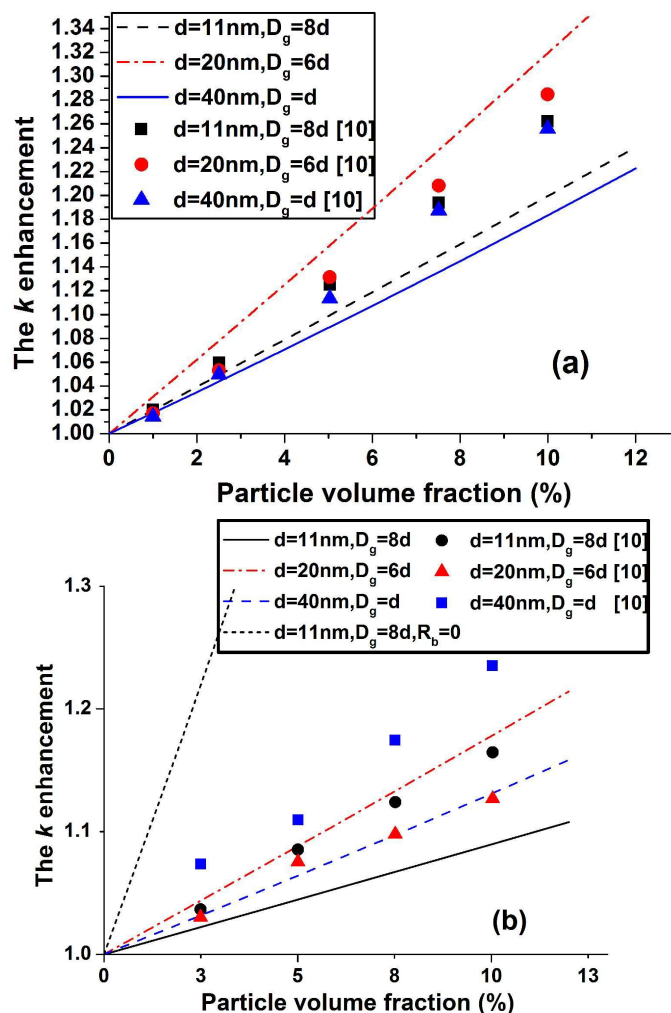
291 The reason why the aggregate size has positive effect on the k enhancement is
 292 that the number of particles in an aggregate increases as aggregate size becomes larger,
 293 which significantly increases the shape factor of aggregate and enhances the k of
 294 nanofluids according to Eq. 8.

295 4.3 Effect of particle volume fraction on the k enhancement

296 The predictions of k enhancement as a function of particle volume fraction for a
 297 series of alumina nanofluids are depicted in Fig. 6. The sizes of particles and
 298 aggregates used in the present model are the same as those measured by Timofeeva et
 299 al.¹⁰ In their experiment, the k of water and ethylene glycol based alumina nanofluids
 300 were measured and aggregate size distribution were determined by DLS. Although the
 301 intensity-weighted distributions of aggregate sizes have two peaks, the volume
 302 fractions of bigger aggregates are much less than that of the smaller ones. Therefore,
 303 the sizes of smaller aggregate are considered as the aggregate sizes, which are 88, 120,
 304 and 40 nm, and the nominal particle diameters are 11, 20, and 40 nm, respectively.

305 It can be seen from Fig.6 that the k enhancement of nanofluids increases linearly
 306 with the rise of particle volume fraction, which is consistent with the experimental
 307 data. For ethylene glycol based nanofluids (Fig. 6(a)), when volume fraction is fixed,
 308 the highest enhancement is observed in nanofluids with particle size of 20 nm, the
 309 second highest for 11 nm particles and the lowest for 40 nm particles. The

310 experimental data are within the range of predictions and show that all particle sizes
 311 present the same trend and this factor less influence on the k enhancement. The reason
 312 why nanofluids with the largest particle size ($d=40$ nm) shows the lowest k
 313 enhancement is that particles ($d=40$ nm) are well dispersed in the base fluid without
 314 aggregation and cannot form rapid thermal conduction path among themselves. By
 315 contrast, for water based nanofluids (Fig. 6(b)), experimental data show that
 316 nanofluids with particle size of 40 nm shows the highest k enhancement, which is not
 317 consistent with the present model. The maximum deviations between the
 318 experimental data and present model are within $\pm 8.5\%$ and the reason might be the
 319 variation of particle size distribution and the uncertainty of interfacial thermal
 320 resistance.



321

322

323 Fig. 6. The k enhancement as a function of particle volume fraction. The lines are the

324 present model predictions of k enhancement for nanofluids with 11, 20, and 40 nm
325 nominal size alumina particles in (a) ethylene glycol and (b) water. The aggregate
326 sizes are four, six and one time (s) of the particle size respectively. The dots are the
327 experimental data from ref. 10.

328 The uncertainty of interfacial thermal resistance has a great influence on the k
329 enhancement, as shown in Fig. 6(b). When interfacial thermal resistance is neglected,
330 the k enhancement is much larger than the prediction with $R_b = 1 \times 10^{-8} \text{ Km}^2/\text{W}$ for
331 water based nanofluids of fixed volume fraction. Although it is hard to obtain the
332 exact value of interfacial thermal resistance, the comparisons between the present
333 model and the experimental data^{7,10,11,34} show that the inferred values of interfacial
334 thermal resistance are in a reasonable range.

335 **4.4 Further discussion about the divergence of the present model and some** 336 **experimental results**

337 The relationship between the k of nanofluids and the particle volume fraction
338 differs in different experimental results. Although the present model analyzes the
339 factors of particle size, aggregate size and interfacial thermal resistance on the
340 divergence of k of nanofluids, some phenomenon still need to be discussed further.

341 First, the anomalous k enhancement at a low particle volume fraction, less than
342 0.1 vol%, can not be predicted by present model. The measured k enhancement
343 (k_{eff}/k_f) of 0.001vol% water based Gold nanofluids is 1.015, as shown in Fig. 3,
344 while the present model predicts almost no k enhancement. Pang⁵⁰ found non-linear
345 enhancement at low concentration and the k of nanofluids was much larger than the
346 prediction when using EMT. The k enhancement at low concentration may
347 dominantly contribute to nano-convection and can be predicted by the model built by
348 Pang et al.³⁷ and Prasher et al.²¹

349 Second, some nanofluids with a small amount of aggregation and particles whose
350 diameter is lower than 10 nm show larger k enhancement than the predictions of the
351 present model. Eastman et al.³⁸ found that k enhancement of ethylene glycol based Cu
352 nanofluids was up to 1.4 when particle volume fraction was 0.3 %. In this study, a

353 one-step production procedure was used and the particle diameter was less than 10 nm
354 with very little aggregate. Philip et al.⁴ reported that the k enhancement of Fe₃O₄
355 nanofluids was larger than the predictions of the present model. The particle diameter
356 was 8 nm and there was little aggregate. The reason why nanofluids without aggregate
357 but with well dispersed particles whose diameter was less than 10 nm show larger k
358 enhancement might result from the forming of the solid-like nanolayer at the
359 solid/liquid interface. The solid-like liquid layer of thickness h around particles is
360 more ordered than that of the base fluid and the k of layer is larger than that of base
361 fluids. The effective particle volume fraction would be calculated as $\phi_{eff} = \phi(1 + h/r)^3$,
362 much larger than the primary particle volume fraction.

363 Third, the present model could not predict the k of nanofluids if the shape of
364 particles is not sphere. The k of alumina nanorods nanofluids is larger than the k of
365 alumina particle at the same particle volume fraction.¹¹ Philip et al.⁴ concluded that all
366 thermal conductivity studies in Carbon nanotube (CNT) nanofluids showed k
367 enhancement is inconsistent with the predictions of EMT. The reason might be that
368 the shape factor of nanorods and CNT are larger than that of the sphere particles.
369 Lamas et al.³⁹ concluded several correlations to predict the k of CNT nanofluids and
370 presented critical analysis on these models. However, it is still necessary to conduct
371 further studies about the influence of the particle shape on the k enhancement.

372 5. Conclusions

373 In the present work, a model for predicting the thermal conductivity of nanofluids
374 is built considering particle size, aggregate size and interfacial thermal resistance. In
375 the present model, the existence of interfacial thermal resistance is considered, and
376 aggregate acts as an independent unit of particle. The shape factor of the aggregate is
377 determined based on the number of particles in the aggregate. The k of nanofluids is
378 obtained by using EMT-based Hamilton model. Based on analysis on the factors that
379 influence the k enhancement, it is concluded that particle size and aggregate size have
380 positive effect on the k enhancement. The increase of particle size can weaken the
381 effect of interfacial thermal resistance and enhance the k of nanofluids because the

382 total surface area of the solid/liquid interface decreases as particle size increases. As
383 aggregate size becomes larger, the shape factor of aggregate significantly increases
384 and the k of nanofluids will also be enhanced. The k of nanofluids increases linearly
385 with particle volume fraction, and the increase rates vary according to particle size
386 and aggregate size. This can explain the divergence of the experimental results. Since
387 present model fits different experimental data well, the inferred values of interfacial
388 thermal resistance are in a reasonable range. Considering the case of nanofluids with
389 particle volume fraction lower than 0.1% and particle size smaller than 10 nm without
390 aggregation, the factors of nano-convection and nanolayer need to be taken into
391 account.

392 **References**

- 393 1. S. U. S. Choi, Z. G. Zhang, W. Yu, F. E. Lockwood, E. A. Grulke, *Appl. Phys. Lett.*,
394 2001, 79, 2252-2254.
- 395 2. S. S. J. Aravinda and S. Ramaprabhu, *RSC Adv.*, 2013, 3, 4199-4206.
- 396 3. Y. Xuan, H. Duan and Q. Li, *RSC Adv.*, 2014, 4, 16206-16213.
- 397 4. J. Philip and P. D. Shima, *Adv. Colloid Interface Sci.*, 2012, 183-184, 30-45.
- 398 5. H. E. Patel, T. Sundararajan and S. K. Das, *J. Nanopart. Res.*, 2010, 12, 1015-1031.
- 399 6. W. Z. Cui, Z. J. Shen, J. G. Yang, S. H. Wu and M. L. Bai, *RSC Adv.*, 2014, 4,
400 55580-55589.
- 401 7. M. P. Beck, Y. H. Yuan, P. Warriar and A. S. Teja, *J. Nanopart. Res.*, 2009, 11,
402 1129-1136.
- 403 8. P. M. Sudeep, J. Taha-Tijerina, P. M. Ajayan, T. N. Narayananc and M. R.
404 Anantharaman, *RSC Adv.*, 2014, 4, 24887-24892.
- 405 9. S. K. Das, N. Putra, P. Thiesen and W. Roetzel, *J. Heat Trans.*, 2003, 125, 567-574.
- 406 10. E. V. Timofeeva, A. N. Gavrilov, et al, *Phys. Rev. E.*, 2007, 76: 061203.
- 407 11. J. Buongiorno, et al, *J. Appl. Phys.*, 2009, 106, 094312.
- 408 12. R. Prasher, W. Evans, P. Meakin, J. Fish, P. Phelan and P. Keblinski, *Appl. Phys.*
409 *Lett.*, 2006, 89, 143119.
- 410 13. P. Keblinski, S. R. Phillpot, S. U. S. Choi and J. A. Eastman, *Int. J. Heat Mass*
411 *Trans.*, 2002, 45, 855-863.
- 412 14. D. Lee, J. W. Kim and B. G. Kim, *J. Phys. Chem. B.*, 2006, 110, 4323-4328.
- 413 15. H. Younes, G. Christensen, X. Luan, H. Hong and P. Smith, *J. Appl. Phys.*, 2012,
414 111, 064308.
- 415 16. J. C. Maxwell, Clarendon Press, Oxford, UK, 1873.
- 416 17. R. L. Hamilton and O. K. Crosser, *Ind. Eng. Chem. Fund.*, 1962, 1, 187-191.
- 417 18. C. J. Yu, A. G. Richter, A. Datta, M. K. Durbin and P. Dutta, *Phys. B.*, 2000, 283,
418 27-31.
- 419 19. W. Yu and S. U. S. Choi, *J. Nanopart. Res.*, 2003, 5, 167-171.
- 420 20. R. Prasher, P. Bhattacharya and P. E. Phelan, *Phys. Rev. Lett.*, 2005, 94, 025901.
- 421 21. R. Prasher, P. Bhattacharya and P. E. Phelan, *J. Heat Transf.*, 2006, 128, 588-595.

- 422 22. S. Mehta, K. P. Chauhan and S. Kanagaraj, *J. Nanopart. Res.*, 2011, 13,
423 2791-2798.
- 424 23. J. W. Gao, R. T. Zheng, H. Ohtani, D. S. Zhu, G. Chen, *Nano lett.*, 2009, 9,
425 4128-4132.
- 426 24. S. P. Jang and S. U. S. Choi, *Appl. Phys. Lett.*, 2004, 84, 4316-4318.
- 427 25. R. Prasher, P. E. Phelan and P. Bhattacharya, *Nano Lett.*, 2006, 6, 1529-1534.
- 428 26. C. W. Nan, R. Birringer, D. R. Clarke and H. Gleiter, *J. Appl. Phys.*, 1997, 81,
429 6692.
- 430 27. W. Evans, R. Prasher, J Fish, et al. *Int. J. Heat Mass Transf.*, 2008, 51, 1431-1438.
- 431 28. G. Okeke, S. Witharana, S. J. Antony, Y. Ding, *J. Nanopart. Res.*, 2011, 13,
432 6365-6375.
- 433 29. D. Q. Zhou and H. Y. Wu, *Appl. Phys. Lett.*, 2014, 105, 083117.
- 434 30. D. P. H. Hasselman and L. F. Johnson, *J. Comp. Materials*, 1987, 21, 508-515.
- 435 31. T. D. Waite, J. K. Cleaver, J. K. Beattiez, *J Colloid Interface Sci.*, 2001, 241,
436 333-339.
- 437 32. B. X. Wang, L. P. Zhou, X. F. Peng, *Int J Heat Mass Transf.*, 2003, 46, 2665-2672.
- 438 33. P. Meakin, *Reviews Geophysics*, 1991, 29, 317-354.
- 439 34. E. V. Timofeeva¹, D. S. Smith, et al., *Nanotechnology*, 2010, 21, 215703.
- 440 35. O. M. Wilson, X. Hu, D. G. Cahill, P. V. Braun, *Phys. Review B.*, 2002, 66,
441 224301.
- 442 36. L. Xue, P. Keblinski, S. R. Phillpot, S. U. S. Choi, and J. A. Eastman, *J.Chem.*
443 *Phys.*, 2003, 118, 337-339.
- 444 37. C. Pang C, J. Y. Jung, Y. T. Kang, *Int. J. Heat Mass Transf.*, 2014, 72, 392-399.
- 445 38. J. A. Eastman, S. U. S. Choi, S. Li, W. Yu, and L. J. Thompson, *Appl. Phys. Lett.*
446 2001, 78, 718-720.
- 447 39. B. Lamas, B. Abreu, A. Fonseca, N. Martins and M. Oliveira, *Int. J. Ther. Sci.*,
448 2014, 78, 65-76.

Interfacial thermal resistance is modeled to have relationship with the equivalent particle size in terms of keeping thermal resistance constant.

